Accuracy analysis of the thrust force in 2D-3D finite element models

G. Deliége
TWR, Katholieke Universiteit Leuven, Heverlee, Belgium, and
F. Henrotte and K. Hameyer
RWTH-Institut für Elektrische Maschinen, Aachen, Germany

Abstract

Purpose – The purpose of this paper is to analyse the accuracy of the thrust force of a linear actuator computed with different finite elements models.

Design/methodology/approach – A series of 2D and 3D models corresponding to different levels of approximation of the original problem are considered. A reliable error estimator based on dual magnetostatic formulations is used.

Findings – A 3D model does not necessarily ensure more accurate results than a 2D model. Because of limitations on the number of mesh elements, the discretisation error in 3D can be of the same order of magnitude as the error introduced by the 2D approximation.

Originality/value – The results emphasise the need to consider errors arising from different simplifications with respect to one another, in order to avoid improvements of the model increasing the complexity but not improving the accuracy of the results.

Keywords Finite element analysis, Force measurement, Electric machines, Actuators, Flux, Transverse waves

Paper type Technical paper

1. Introduction

The finite element (FE) method is a versatile and powerful numerical method for the solution of partial differential equations. It is widely used for the numerical analysis of electrical devices. In general, obtaining a solvable FE model requires several simplifications of the original physical system, in order to reduce its complexity. Approximations can be made on a rigorous basis. One can for instance eliminate negligible terms in an equation on basis of a dimensional analysis. However, the loss of accuracy resulting from simplifications is in general difficult to quantify. The influence of the 2D approximation on global quantities like energy or the force is very sensitive to the geometry of the studied system. This paper proposes an analysis of the accuracy of the force computed with different FE approximations of a linear actuator. The goal is to determine a FE model that minimises the computation time, but nevertheless yields sufficiently accurate results, so that it could be used to perform an optimisation of the device.

After a brief description of the actuator, a series of models (2D and 3D) corresponding to different levels of approximation of the original problem are

This text presents results of the Belgian programme on Interuniversity Poles of Attraction initiated by the Belgian State, Prime Minister's Office, Science Policy Programming.

COMPEL: The International Journal for Computation and Mathematics in Electrical and Electronic Engineering
Vol. 25 No. 2, 2006
pp. 320-333

0332-1649
DOI 10.1108/03321640610649005

considered. The dual vector potential a and scalar potential ϕ formulations in 2D and 3D are recalled. Appropriate boundary conditions for the different models are discussed. An error estimator based on the results of these dual formulations is then defined. Two force computation methods are used: the direct finite differentiation of energy or coenergy, and the eggshell method.

2. Description of the motor

The actuator has been described in detail in previous papers (Vande Sande *et al.*, 2002; Deliége *et al.*, 2003). It consists of two identical linear motors facing each other (Figure 1). The stators are long C-cores with a coil wound around the vertical arm. The lower and upper arms are toothed in such a way that the stator of one motor is shifted by a quarter of a pole pitch with respect to the stator of the other one. The equivalent to the rotor is here called mover. Each mover consists of a stack of five blocks: a permanent magnet block magnetised along the X-direction, a block of iron, a second permanent magnet block magnetised along the $-X$-direction, a second iron block and finally a third permanent magnet block again magnetised along the X-direction. The movers of the two motors are fixed on both sides of a piece of non-magnetic material of the same length as the movers, in order to avoid any magnetic interaction between the two motors. The actuated optical system is fixed to that central piece. As they are magnetically independent, only one motor need to be considered in the FE model.

3. Geometric simplifications

Originally, the aim of this FE analysis was the optimisation of the force acting on the mover. Under certain conditions, a simple magnetic equivalent circuit can describe the flux distribution in a permanent magnet machine with a sufficient accuracy and give a good approximation of the thrust force at a low computation cost (Honds and Meyer, 1982). In transverse flux machines, the intricate geometry makes such an approach impossible (Laithwaite *et al.*, 1971). The FE method is in that case the best alternative: it is flexible regarding the approximation of the geometry, and the accuracy can be controlled by user-defined parameters, such as the number of elements in the mesh.

3.1 Airgap-centred 3D model

The basis model consists of one linear actuator (one half of the whole device) enclosed in an air box, inside which the magnetic flux is assumed to be confined. As most of the

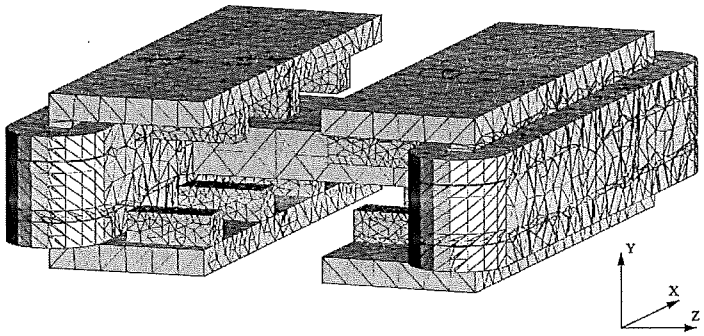

Figure 1.
Geometry of the linear actuator

flux remains in the regions of high permeability, i.e. the iron parts of the stator and rotor, the surrounding air box needs only to be large enough to allow leakage fluxes in the airgap to be modelled. The enclosing box can, therefore, be placed quite close to the structure.

On the other hand, the regions in the model where the flux paths are predictable should advantageously be left out of the model and replaced by an equivalent external magnetic circuit (Figure 2), so as to spare the unknowns used to describe them. In this particular application, the vertical arm of the stator and the coil around it can be left outside the FE model, because the accuracy of the computed force depends on the accuracy of the field in the airgap. This geometrical simplification, called airgap-centred 3D model, devotes a maximum of the available unknowns to the description of the field around the mover. The equivalent external circuit would consist in this case of a reluctance and a current source. However, due to the presence of large airgaps and magnets, the external reluctance is negligible. The excitation of the actuator can, therefore, be included in the boundary conditions, as will be explained further.

3.2 2D model

The 3D effects around the mover can of course not be estimated by a 2D analysis. However, 2D models has definite advantages when compared to a complete 3D model: the definition of the geometry and the control of the mesh quality are much easier and faster, the computational resources needed are much smaller. In total, the overall modelling time is generally orders of magnitude lower. Therefore, it is always worth using a 2D model as a preliminary step. This allows the designer to perform numerous and various computations, in order to determine the overall behaviour of the system and to investigate the influence of the parameters, at a reduced computation cost. The 2D simplified model used in this paper is a slice of the motor in the *XY*-plane (Figure 3). Two regions are added, above and under the stator teeth, to represent the horizontal upper and lower arms of the stator.

4. Finite element formulations

The dual vector potential and scalar potential formulations will be referred to as *b*- and *h*-formulation, respectively. These formulations provide, respectively, an upper and a lower bound for the magnetic energy (Rikabi *et al.*, 1988, 1989). The actual error on energy is thus smaller than the difference between the values computed with the dual formulations.

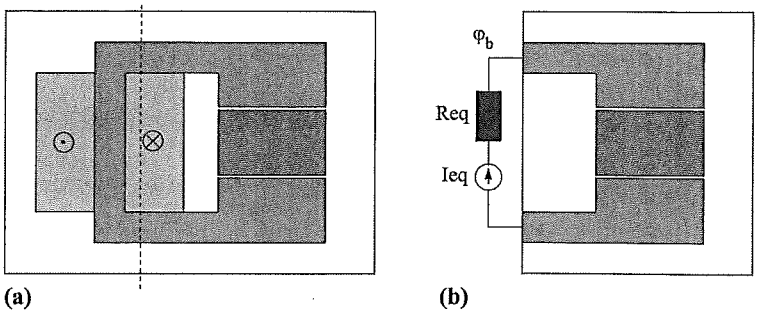

Figure 2.
Coil modelling (a) explicit definition in the geometry; and (b) equivalent magnetic circuit

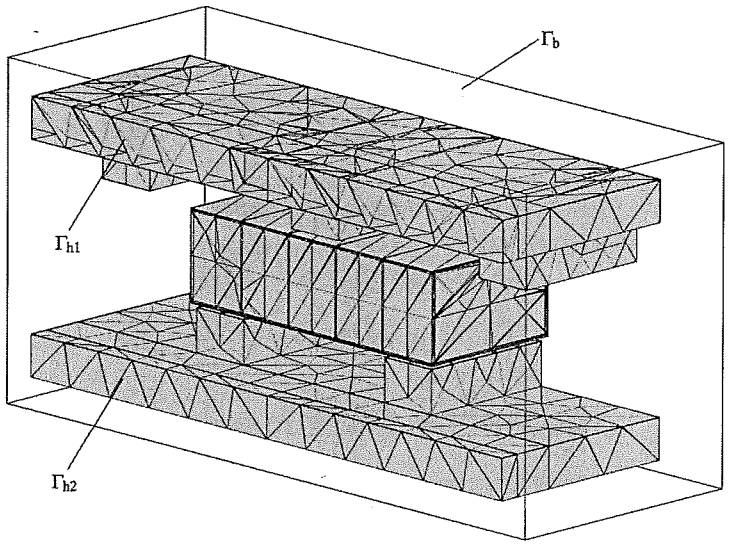

Figure 3.
Boundaries of the 3D model; Γ_b includes all boundaries except Γ_{h1} and Γ_{h2}

4.1 Boundary conditions

The airgap-centred model can be regarded as an open section of a magnetic circuit. Particular boundary conditions must be defined to account for the magnetisation coil, which is not explicitly modelled in the geometry. The alternatives are to fix either the drop of the magnetomotive force I across the section, or the flux φ_b injected in the circuit. The former is naturally imposed with a Dirichlet conditions in a h-formulation, whereas the latter is fixed in a b-formulation. However, the flux is not a given variable of the problem. Therefore, the h-formulation will be solved first and the results will be used to calculate the value of φ_b for the b-formulation (Figure 4).

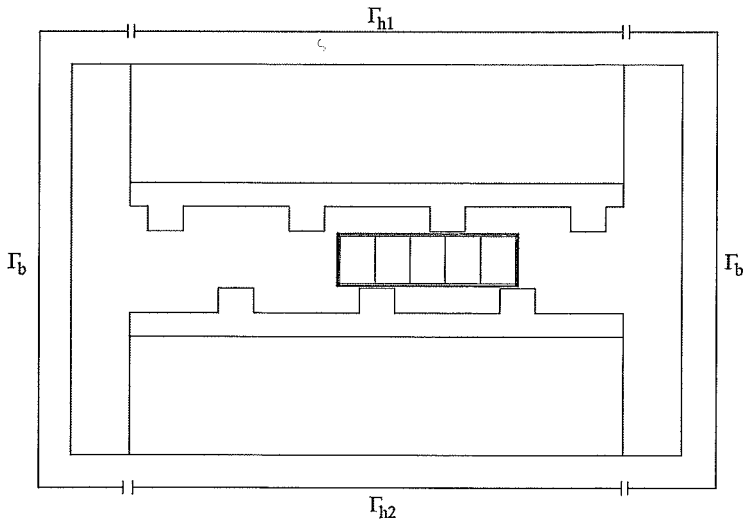

Figure 4.
Boundaries of the 2D model

4.2 h-formulation

The magnetic field is usually decomposed into the sum of a source field $\underline{h}_s$ and the gradient of a magnetic scalar potential ϕ:

$$\underline{h} = \underline{h}_s - \nabla\phi \tag{1}$$

Since the coil is removed from the geometrical model, the source current density j is zero, and $\underline{h}_s$ is zero as well thanks to the fact that the domain is contractible (Bossavit, 1998). The magnetic constitutive law is:

$$\underline{b} = \mu(\underline{h} + \underline{h}_c), \tag{2}$$

with $\underline{h}_c$ the remanent magnetic field, which is zero outside the permanent magnet regions. The boundary conditions are:

$$\phi|_{\Gamma_{h1}} = 0, \quad \phi|_{\Gamma_{h2}} = I, \quad (\mu\nabla\phi|_{\Gamma_b})\underline{n} = 0. \tag{3}$$

The FE formulation reads:

Find $\phi \in H_\phi(\Omega)$ such that:

$$\int_\Omega \mu\nabla\phi' \cdot \nabla\phi = \int_\Omega \mu\nabla\phi' \cdot \underline{h}_c, \tag{4}$$

$\forall\phi' \in H_{\phi 0}$, with the function spaces:

$$H_\phi(\Omega) = \{\phi \in H(\text{grad}, \Omega) : \phi|_{\Gamma_{h1}} = 0, \phi|_{\Gamma_{h2}} = I\}, \tag{5}$$

$$H_{\phi 0}(\Omega) = \{\phi \in H(\text{grad}, \Omega) : \phi|_{\Gamma_{h1} \cup \Gamma_{h2}} = 0\}. \tag{6}$$

4.3 b-formulation

The vector potential $\underline{a}$ is by definition such that $\underline{b} = \nabla \times \underline{a}$. The flux φ_b is fixed by the boundary conditions:

$$\int_{\partial\Gamma_{h1}} \underline{a} \cdot \underline{t}\, \mathrm{d}\partial\Gamma = \varphi_b, \quad \nabla \times \underline{a}|_{\Gamma_b} \cdot \underline{n} = 0, \tag{7}$$

where $\underline{t}$ is the vector tangent to the contour of Γ_{h1}. The formulation reads:
Find $\underline{a} \in H_a(\Omega)$ such that:

$$\int_\Omega \mu^{-1}\nabla \times \underline{a}' \cdot \nabla \times \underline{a} = \int_\Omega \nabla \times \underline{a}' \cdot \underline{h}_c, \tag{8}$$

$\forall \underline{a}' \in H_{a0}$, with the function spaces:

$$H_a(\Omega) = \left\{\underline{a} \in H(\text{curl}, \Omega) : \nabla \times \underline{a}|_{\Gamma_b} = 0, \int_{\partial\Gamma_{h1}} \underline{a} \cdot \underline{t} = \varphi_b\right\} \tag{9}$$

$$H_{a0}(\Omega) = \left\{\underline{a} \in H(\text{curl}, \Omega) : \underline{a}|_{\Gamma_b} = 0, \underline{a}|_{\partial\Gamma_{h1}} = 0\right\} \tag{10}$$

Building a discretised equivalent of the constrained function space $H_a(\Omega)$ is not straightforward. One possible method consists in building a spanning edge-tree

on $\Gamma_b \cup \partial\Gamma_{h1}$. That spanning tree must, moreover, contain a tree on the contour $\partial\Gamma_{h1}$ (Henrotte and Hameyer, 2003). In other words, all edges of $\partial\Gamma_{h1}$ but one must belong to the tree. The degrees of freedom of $\underline{a}$ are cancelled on the edges of the tree and the remaining degrees of freedom, associated with the edges of the co-tree, are determined so as to fulfil the condition (7) on all faces of Γ_b. Figure 5 shows the resulting vector potential field on the boundary $\Gamma_b \cup \partial\Gamma_{h1}$.

4.4 Energy, coenergy, complementary energy

Assuming linear materials, the energy $\Psi(\underline{b})$, the co-energy $\Phi(\underline{h})$ and the complementary energy $\Psi_c(\underline{h})$ are defined by equation (11):

$$\Psi(\underline{b}) = \int_\Omega \left(\frac{1}{2\mu}\underline{b}\cdot\underline{b} - \underline{b}\cdot\underline{h}_c\right)\mathrm{d}\Omega$$

$$\Phi(\underline{h}) = \int_\Omega \frac{\mu}{2}(\underline{h}+\underline{h}_c)^2\mathrm{d}\Omega \tag{11}$$

$$\Psi_c(\underline{h}) = \int_\Omega \mu\underline{h}\cdot(\underline{h}+\underline{h}_c)\mathrm{d}\Omega - \Phi(\underline{h})$$

These formulae are written in the general case of a permanent magnet material with a remanent magnetic field $\underline{h}_c$. The quantities $\Psi(\underline{b})$ and $\Psi_c(\underline{h})$ are equal only if the FE solution corresponds to the exact solution.

5. Force computation

The FE computation of the magnetic force acting on a body is a difficult issue, as shown by the considerable amount of research devoted to it (Bossavit, 1990, 1992; Henrotte *et al.*, 2004). For this paper, an accurate method that could be applied to the 2D and 3D models and for dual formulations was necessary. Two techniques were used: the direct differentiation of energy and the eggshell method (Henrotte *et al.*, 2004).

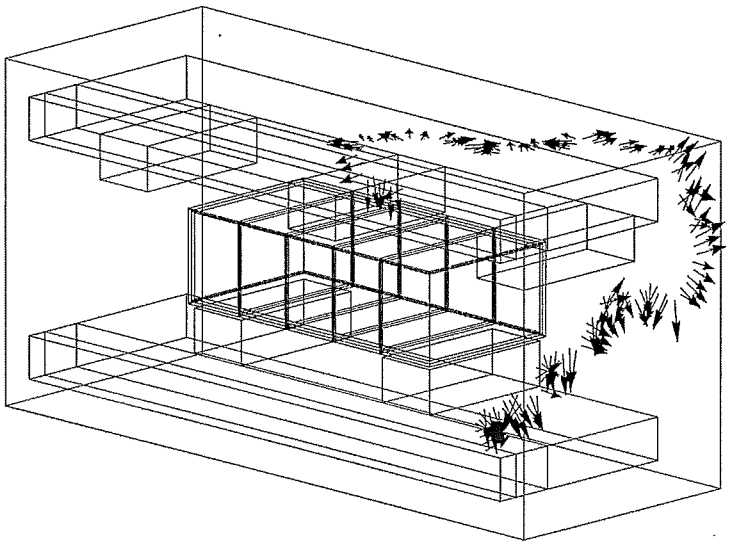

Figure 5.
Vector potential a on the boundary, such that its line integral on $\partial\Gamma_{h1}$ equals φ_b and curl(a).n = 0 on Γ_b

5.1 Energy differentiation

The thrust force acting on the mover in one direction is equal to the derivative of the total magnetic energy or coenergy of the system with respect to the displacement in the considered direction. However, the analytical expression of Ψ and Φ as a function of the position of the mover x_p is unknown. Therefore, these quantities must be derived numerically. A second order accurate value of the force in the X-direction is given by equation (12):

$$F_x(x) = \frac{\Psi(\underline{b})|_{x_p=x+\delta x} - \Psi(\underline{b})|_{x_p=x-\delta x}}{2\delta x} = -\frac{\Phi(\underline{h})|_{x_p=x+\delta x} - \Phi(\underline{h})|_{x_p=x-\delta x}}{2\delta x} \tag{12}$$

One drawback of this approach is that it requires several solutions at different positions, located close together enough to ensure the accuracy of the results. Moreover, this procedure must be repeated for each component of the force. For example, six FE solutions are required to determine the values of F_x, F_y and F_z at one position with equation (12). This is, however, not a hindrance in the present case: on the one hand, the force is only computed in the direction of motion; and on the other hand, the force profile must be determined over the entire stroke of the mover, which means that the solution has to be computed at many different positions anyway.

5.2 The eggshell method

The eggshell method (Henrotte *et al.*, 2004) states that the magnetic force $\underline{F}$ acting on a rigid body can be evaluated by a volume integral over an air shell Ω_c placed around the moving body (Figure 6). One has:

$$\underline{F} = \int_{\Omega_c} \underline{\underline{\sigma}}_M \cdot \nabla u \, d\Omega_b \tag{13}$$

where $\underline{\underline{\sigma}}_M$ is the Maxwell stress tensor (MST) of air, and u is any smooth scalar function defined on Ω_c, whose value is 1 on the inner boundary of the shell and 0 on the outer boundary. If the contribution of the electric force is negligible, the MST is expressed as a function of $\underline{b}$ or $\underline{h}$ by, respectively:

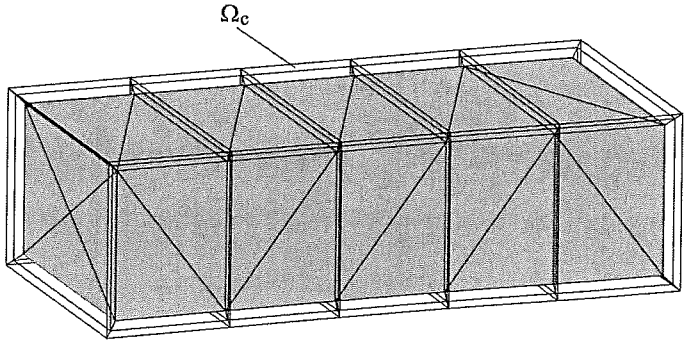

Figure 6.
Eggshell region around the mover in the 3D model

$$\underline{\underline{\sigma}}_M(\underline{b}) = \frac{1}{\mu_0}\left(\underline{b}\otimes\underline{b} - \frac{1}{2}(\underline{b}\cdot\underline{b})\underline{\underline{I}}\right), \qquad (14)$$

$$\underline{\underline{\sigma}}_M(\underline{h}) = \mu_0\left(\underline{h}\otimes\underline{h} - \frac{1}{2}(\underline{h}\cdot\underline{h})\underline{\underline{I}}\right).$$

In the particular case where u varies linearly on the eggshell, the method can be given a simple interpretation, as shown in Figure 7. The isovalues of u determine in Ω_c a family $\Gamma_b(u)$ of concentric enclosing surfaces. They fill up the volume Ω_c as the parameter u ranges from 0 to 1. The force acting on Ω_b can be obtained by integrating the MST on any of those surfaces. Since the calculated force is in theory independent of the chosen integration surface, the force is also equal to the mean of the values obtained by integrating on all surfaces, so that one has:

$$\underline{F} = \int_0^{\delta}\frac{1}{\delta}\int_{\Gamma_b(u)}\underline{\underline{\sigma}}_M\cdot\underline{n}\,\mathrm{d}\Gamma_b\,\mathrm{d}u = \int_{\Omega_c}\underline{\underline{\sigma}}_M\cdot\nabla u\,\mathrm{d}\Omega_c \qquad (16)$$

because $\nabla u = \underline{n}/\delta$, due to the linearity of u. The surface integral is in this way replaced with an integral on a volume. The eggshell Ω_c can be explicitly defined in the geometrical model or automatically. Figure 7 shows the eggshell in the 3D FE model. It has a constant thickness. It consists of the space bounded by two concentric parallelepipeds, subdivided into six subregions in which the normal vector $\underline{n}(u)$ is constant and, therefore, easy to define.

6. Results

6.1 2D results

The 2D problem was first solved for a single position of the mover corresponding to a maximum of the delivered force. The computation was repeated with different meshes obtained by globally refining an initial mesh of 2,800 nodes until it reached 40,000 nodes. The energy and complementary energy converge towards each other as predicted by theory (Figure 8). The forces computed on basis of the scalar potential and vector potential formulations converge towards each other in a similar way (Figure 9). However, the error on the force is significantly higher than the error on the energy (Table I).

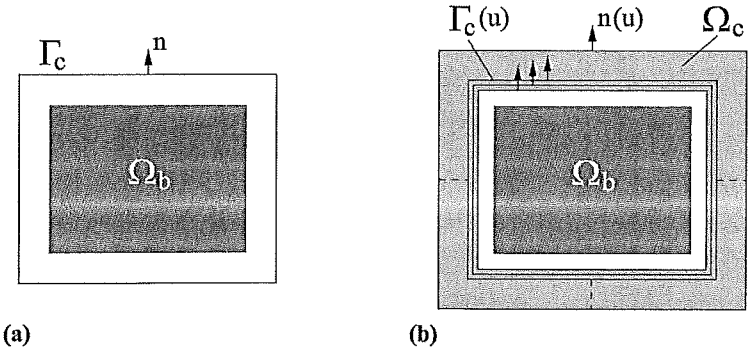

Figure 7.
Illustration of (a) the MST method (integration on one enclosing surface); and (b) the eggshell method

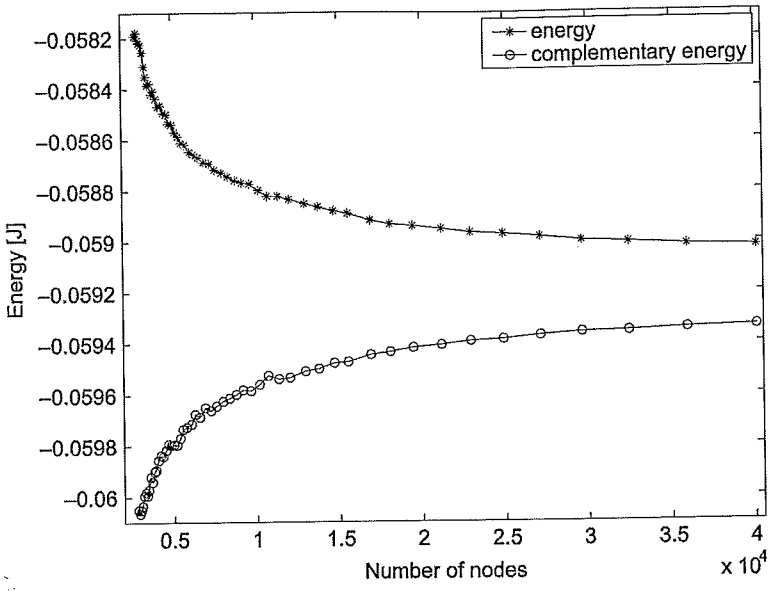

Figure 8.
Convergence of the total energy and the complementary energy; 2D model, $xp = 0.125$ pole pitches, $I = 0$

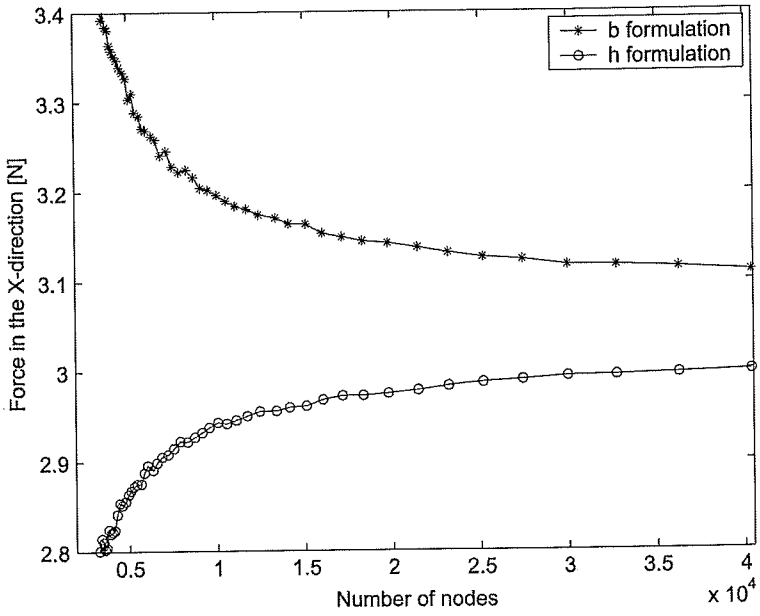

Figure 9.
Convergence of F_x computed with the eggshell method; 2D model, $\underline{b}$ and $\underline{h}$ formulations, $xp = 0.125$ pole pitches, $I = 0$

This does not result from the method used to compute the force since identical values are obtained with the eggshell method and by differentiation of the energy, when computed with the same formulation (Figure 10). Actually, the error on the force converges like the error on the energy and coenergy, but simply remains one order of magnitude higher; as shown in Figure 11 where the evolution of the respective errors is

plotted on a
model have
induction, w
However,
influence glo
linear and nc

- A grid
  accurac
  than tw
- The err
  4 per ce
- Non-line
  example
- The egg
  formulat
  purpose

Nb nodes
28,000
40,000

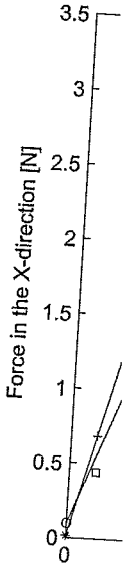

plotted on a log-log scale. The results computed with a linear model and a non-linear model have also been compared. There is a noticeable difference in the values of the induction, which reaches 2.3 T in the corners of the teeth with the linear model.

However, saturation is confined to small areas of the motor and does hardly influence global quantities: for example, F_x differs by no more than 0.5 per cent in the linear and non linear cases. In summary, one can state:

- A grid of 20,000 to 25,000 nodes is for this model a good trade-off between accuracy and computation time. The mesh in the eggshell does not need more than two or three layers of elements.
- The error on the maximum delivered force stands in that case between 3 and 4 per cent.
- Non-linear computation brings a difference of 0.5 per cent and is in the studied example superfluous.
- The eggshell method is reliable, easily implemented and it applies to $\underline{b}$ and $\underline{h}$ formulations in 2D and 3D; it appears, therefore, as an ideal method for the purpose of computing global forces.

Table I.
Maximum error on the force and energy and 2D model, two different meshes

Nb nodes	Error (energy) (per cent)	Error (force) (per cent)
28,000	3.2	18
40,000	1.8	3.6

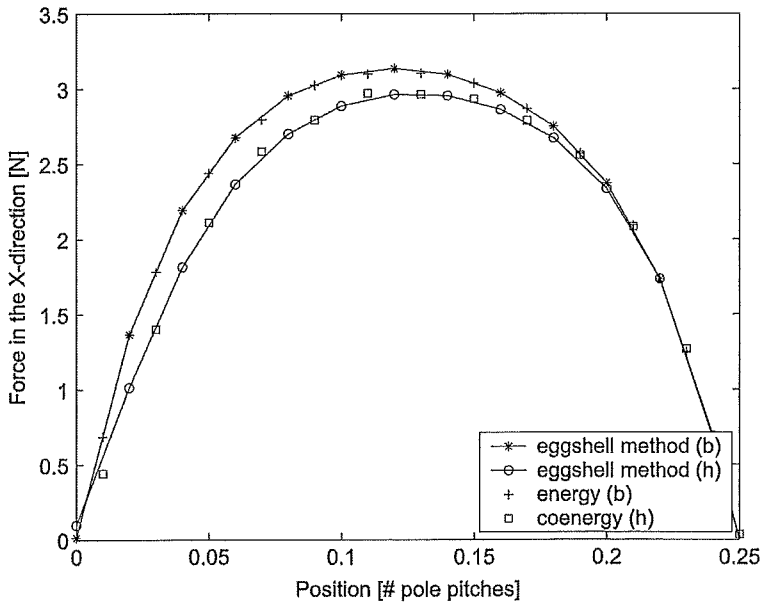

Figure 10.
Comparison of the force computed by the eggshell method and the differentiation of the energy and coenergy; 2D model, xp ranges from 0 to 0.5 pole pitches, $I = 0$

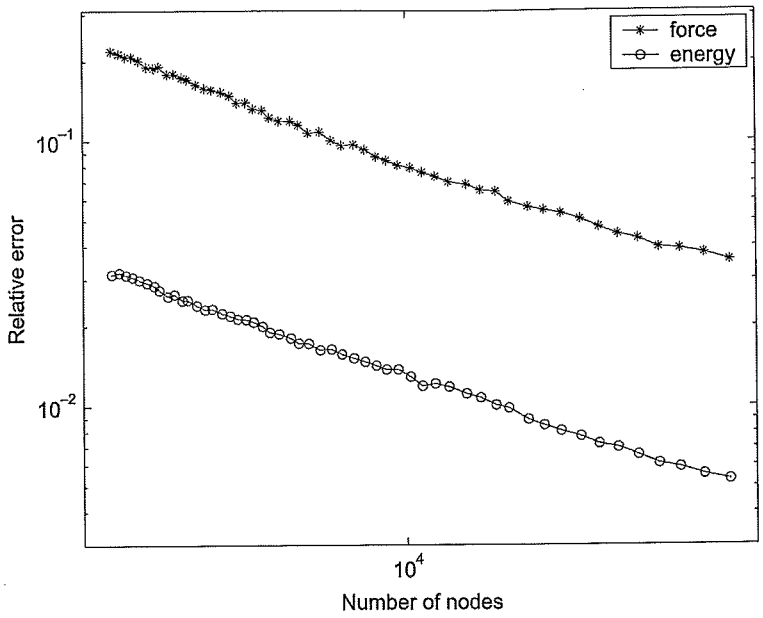

Figure 11.
Error convergence of the energy and the force; 2D model, $\underline{b}$ and $\underline{h}$ formulations, $xp = 0.125$ pole pitches, $I = 0$

6.2 3D results

The realisation of the 3D model was a more tedious and delicate task. The airbox modelled around the mover is extremely flat because of the tiny airgap (0.4 mm). As a consequence, the characteristic lengths of the elements of the mesh have to be carefully balanced. The solid modeller comes up against severe difficulties when the grid is too coarse near the flat regions, but a local increase of the number of elements propagates to the whole domain and can result in a prohibitive number of elements. Therefore, the error convergence could not be studied by globally refining the mesh, as it was done for the 2D model, and a single mesh with 350,000 elements has been considered.

The force in the X-direction computed for $I = 200$ A with both formulations is plotted on Figure 12 as a function of the mover's position. The difference between the two curves reaches 26 per cent of the maximum value. In order to compare the 2D and 3D results, the mean of the forces calculated with the $\underline{b}$ and $\underline{h}$ formulations is plotted on Figure 13. It shows that 3D effects have a non-negligible influence on the force, which is overestimated by the 2D model. However, the latter captures the most important features at a much lower computational cost and with a much smaller discretisation error.

7. Conclusions

The FE analysis of a transverse flux linear actuator has been presented. An analysis of the accuracy of the thrust force computed with a 2D and a 3D model has been carried out. A reliable global error estimator based on the results obtained with the dual $\underline{a}$ and $\underline{h}$-ϕ magnetostatic formulations has been considered. Two force computation methods has been used and compared. The eggshell

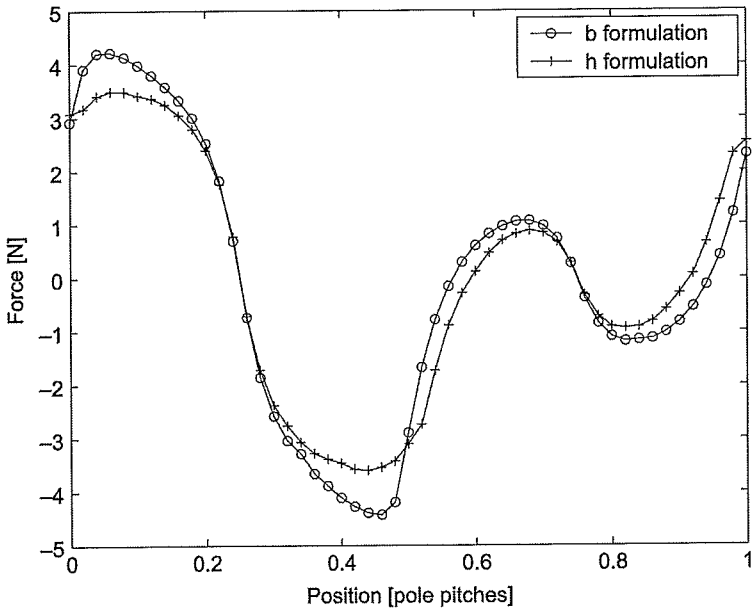

Figure 12.
Force F_x computed with the $\underline{b}$ and $\underline{h}$ formulations; 3D model, xp ranges from 0 to 1 pole pitch, $I = 200$ A

method has proven to be accurate and easy to use. The convergence of the error on energy and on force has been studied in 2D. It has been shown that, although both quantities have the same rate of convergence, the error on the force is one order of magnitude higher than the error on the energy, which is generally taken as a reference for the global accuracy of the model. In 3D, the error reaches a peak value of 26.per cent, proving that the mesh of 350,000 elements is too coarse despite the presence of several layers of elements in the airgap. The comparison of the force profiles computed in 2D and 3D shows that the shape of the curves and the influence of the currents are qualitatively well described by the 2D model, at a much lower computational cost and with a much better continuity. A 3D analysis cannot be avoided because of the important role played by the 3D effects in this application. The force computed by the 2D analysis is indeed overestimated. However, the results suggest that one can pursue quite far the geometrical optimisation with the 2D model, and that the resulting optimum configuration will not be very different from the real optimum. Moreover, the improvement expected from using a non-linear model, is in this case completely lost in view of the general error level.

On the whole, these results confirm the importance in a FE analysis of a careful approach, tackling the problem from different angles. They also emphasize the necessity to consider errors arising from different simplifications with respect to one another, in order to avoid improvements of the model increasing the complexity but not improving the accuracy of the results. In particular, a 3D model does not necessarily ensure more accurate results than a 2D model. Indeed, if the number of mesh elements is limited, the discretization error in the 3D model can be of the same order of magnitude as the error introduced by the 2D approximation.

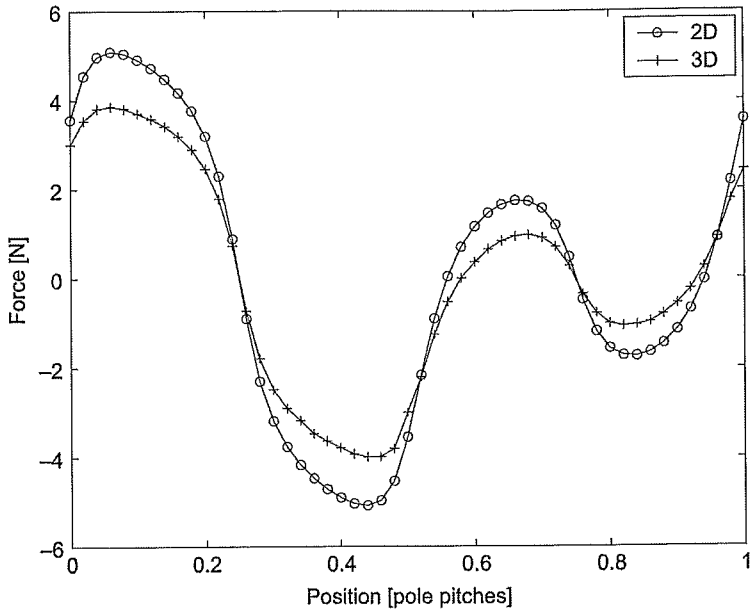

Figure 13.
Comparison of the forces computed with the 2D and 3D models; xp ranges from 0 to 1, mean of the $\underline{b}$ and $\underline{h}$ formulations, $I = 200$ A

References

Bossavit, A. (1990), "Forces in magnetostatics and their computation", *Journal of Applied Physics*, Vol. 67 No. 9, pp. 5812-4.

Bossavit, A. (1992), "Edge element computation of the force field in deformable bodies", *IEEE Transactions on Magnetics*, Vol. 28 No. 2, pp. 1263-6.

Bossavit, A. (1998), *Computational Electromagnetism*, Academic Press, Maryland.

Deliége, G., Henrotte, F., Vande Sande, H. and Hameyer, K. (2003), "3D h-phi finite element formulation for the computation of a linear transverse flux actuator", *International Journal for Computation and Mathematics in Electrical and Electronic Engineering (COMPEL)*, Vol. 22 No. 4, pp. 1077-88.

Henrotte, F. and Hameyer, K. (2003), "An algorithm to construct the discrete cohomology basis functions required for magnetic scalar potential formulations without cuts", *IEEE Transactions on Magnetics*, Vol. 39 No. 3, pp. 1167-70.

Henrotte, F., Deliége, G. and Hameyer, K. (2004), "The eggshell approach for the computation of electromagnetic forces in 2D and 3D", *International Journal for Computation and Mathematics in Electrical and Electronic Engineering (COMPEL)*, Vol. 23 No. 4.

Honds, L. and Meyer, K.H. (1982), "Een lineaire gelijkstroommotor met permanente magneten", Technical report, Philips.

Laithwaite, E.R., Eastham, J.F., Bolton, H.R. and Fellows, T.G. (1971), "Linear motors with transverse flux", *IEE Proceedings*, Vol. 118 No. 12, pp. 1761-7.

Rikabi, J., Bryant, C.F. and Freeman, E.M. (1988), "Error-based derivation of complementary formulations for the eddy current problem", *IEE Proceedings*, Vol. 135 No. 4, pp. 208-16.

Rikabi, J., Bryant, C.F. and Freeman, E.M. (1989), "Complementary solutions of electrostatic field problems", *IEEE Transactions on Magnetics*, Vol. 25 No. 6, pp. 4427-42.

Vande Sande, H., Deliége, G., Hameyer, K., Van Reusel, H., Aerts, W. and De Coninck, H. (2002), "Design of a linear transverse flux actuator", paper presented at the 15th International Conference on Electrical Machines (ICEM), Brugge.

Corresponding author
G. Deliége can be contacted at: geoffrey.deliege@cs.kuleuven.ac.be